2019 SAUPEC/RobMech/PRASA Conference
Bloemfontein, South Africa, January 28-30, 2019

Robust Torque Ripple Mitigation of a Line-Start PMSM by Means of the Taguchi Method

A. J. Sorgdrager and R-J. Wang
Dept. of Electrical & Electronic Engineering
Stellenbosch University
Stellenbosch, South Africa
ajsorgdrager@gmail.com, rwang@sun.ac.za

A. J. Grobler
School of Electr., Electron. & Computer Engineering
North-West University
Potchefstroom, South Africa
Andre.Grobler@nwu.ac.za

***Abstract*—In this paper, a robust design framework is proposed to mitigate torque ripple for line-start permanent magnet synchronous machines (LS-PMSM) by using the Taguchi method. The framework is intended for fine-tuning initial optimum designs to further improve the steady-state torque quality of LS-PMSMs. The proposed framework was successfully implemented on an LS-PMSM design. A notable decrease in steady-state torque ripple was achieved without a significant reduction in steady-state performance and transient load synchronization capability. It has been shown that the proposed robust torque ripple mitigation framework is both functional and time efficient and can be applied to a wide range of electrical machines.**

***Index Terms*—Line start, permanent magnet synchronous machines, torque ripple, robust design, optimization, Taguchi method, finite element analysis**

I. Introduction

Unlike conventional permanent magnet (PM) motors, a line-start PM synchronous motor (LS-PMSM) has a hybrid rotor containing both a squirrel cage and a PM array. This provides self-starting capability and enables synchronous operation at steady-state. Fig. 1 shows the cross-section of a typical LS-PMSM with the PM (in yellow) located below the cage (shown in dark grey). While LS-PMSMs operate similar to a PM synchronous machines at steady-state, they are more prone to severe pulsating torque. This is due to their anisotropic rotor magnetic structure and the electromagnetic interaction between the rotor and stator's respective magnetic flux producing components [2]–[4]. These torque ripples are highly undesirable as they can cause mechanical vibrations, audible noise and premature bearing failures [2]. Although extensive research has been done on LS-PMSMs, very little focus has been placed on their steady-state torque quality aspects.

Since the common torque ripple reduction method like skewing cannot be easily implemented for PM rotor, designers often resort to design techniques such as optimizing rotor geometry [2], [3], slot shaping and position adjustments [5], [6] or introducing flux guides [7]. More recent work also investigated the impact that manufacturing imperfections have on the torque ripple variance [3]. For torque ripple calculations, both analytical and finite element analysis (FEA) have been utilized. Considering the localized magnetic saturation commonly found in interior PM rotors, the analytical methods

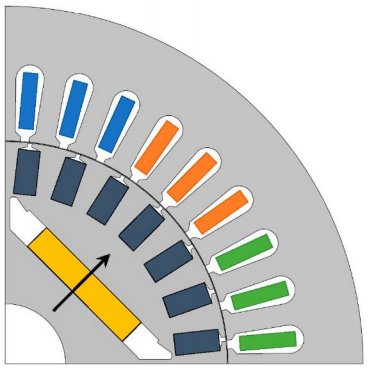

Fig. 1. Radial flux LS-PMSM design from [1].

do not have the required accuracy. Thus, FEA is the preferred method to determine torque characteristics [6] and is particularly compelling when combined with an iterative design optimization framework [3], [5]. However, FEA based torque characteristics calculation can be computationally expensive, especially when used in a design optimization environment [2], [8].

In this paper, a robust design framework is proposed for mitigating torque ripples of LS-PMSMs using the Taguchi method. The intended use of the method is to minimize the ripple torque of an initial optimum LS-PMSM design with minimal impact on its main performance parameters.

The paper is structured as follows: The functionality and the formulation of the robust framework are described in Section II. The implementation of the proposed method on an existing LS-PMSM is presented in Section III. Section IV compares the torque quality between the original and the final machines along with the Taguchi performance plots. From this relevant conclusions are drawn in Section V.

II. Robust Torque Ripple Mitigation Framework

The use of the Taguchi method in electrical machine design is relatively new [9]. The Taguchi method differs from commonly used optimization methods in that it analyses the results to locate a region where the performance objective is most stable rather than searching for a definite point in the domain [1], [10]. Some distinct features of the Taguchi method are

978-1-7281-0369-3/19/$31.00 ©2019 IEEE

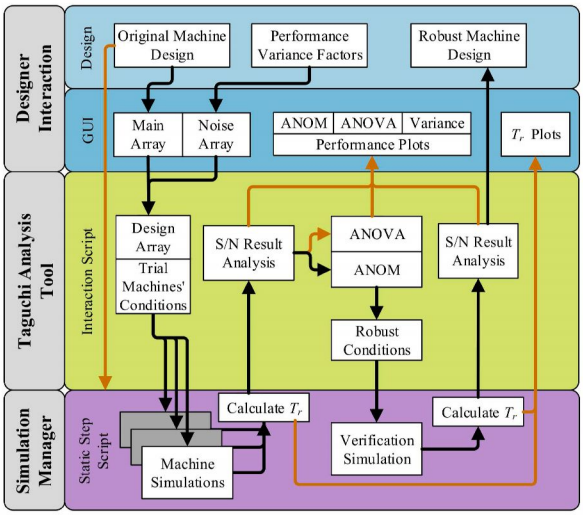

Fig. 2. Functional breakdown of Taguchi torque ripple mitigation framework.

the independence from initial conditions, reduced parameter complexity, and relative ease with determining the subsequent conditions of the parameters in an iterative process.

Some recent work on the use of the Taguchi method for torque ripple minimization of interior PM machines can be found in [6]–[8], [11]–[13]. The basic approach followed was to fine-tune an existing design by either changing the rotor/stator geometry in the air-gap region or altering the profile and position of flux barriers. The sensitivity of pulsating torque components to the variance in material properties and manufacturing tolerance was investigated in [3] and [13]. In the latter the Taguchi method was used to realize a design insensitive to magnetic asymmetry in the design.

In this section, a torque ripple minimization design framework making use of the Taguchi method is described. The diagram and functional breakdown of the proposed design framework is given in Fig. 2, which consists of three function blocks, namely, *Designer Interaction, Taguchi Analysis Tool* and a script-based *Simulation Manager* block.

A. Designer Interaction

The function block houses two parts, namely, the design input/output and graphical user interface (GUI).

• ***Design:*** The designer selects the design variables from the initial optimum machine and set their respective design ranges. Secondly, performance variance factors that directly influence the performance objective are selected and their respected ranges or states defined. For this particular study, the objective is to minimize the torque ripple.

• ***Graphical User Interface:*** The GUI contains the selected main orthogonal array (OA) and outer noise OA. The required OAs are influenced by the number of design and noise parameters. The designer inputs the design variables and their respective ranges in the OA to populate the require OA level set for the design array. Once the Taguchi analysis is completed, the analysis of mean (ANOM) and variance (ANOVA) and trial variance results are presented as performance graphs. The information obtained from each is discussed in Section IV.

B. Taguchi Analysis Tool

The Taguchi Analysis Tool comprising of the *Design Array, Result Analysis* and *Result Processing* is used to identify and confirm the *Robust Conditions*. The in-depth functionality of the Taguchi method is covered in [10] and only the high-level functionality is discussed in this paper.

• ***Design Array and Trial Machines:*** The number of main trial machines are dependent on the selected main OA. The number of noise trials of the main trial machine is dependent on the selected noise OA. Considering that all OA trial states are predefined, the use of parallel processing can be utilized to reduce the overall analysis time required. The trial conditions are fed into the Simulation Manager through an automated script-based protocol.

• ***S/N Result Analysis:*** The trial results of each design array is obtained from the Simulation Manager. The noise trials of each main trial are combined using a specific quality characteristic (QC). As the aim for this study is to minimize the torque ripple (T_r), the *Smaller-is-better* QC is used to calculate the mean squared deviation (MSD) of the performance objective. The MSD is then converted to the S/N ratio of the given main trial. This conversion is what enables the Taguchi method to analyze the results and identify the robust parameters that are insensitive to the selected noise conditions. The main trial S/N ratio can be converted back to a single performance objective that represents the combined performance. Each of the converted performance values is used to compile the trial variance plots showing the rate of change as a function of a parameter change.

• ***ANOVA and ANOM:*** Using the S/N main trial ratios, the ANOM and ANOVA values are calculated as explained in [10]. The ANOM is used to identify the robust conditions of each parameter by studying the main effects of each level, which indicates the performance trend over the parameter range. The ANOVA is a statistical tool used to determine the influence each parameter has on the performance outcome. Once the optimum level conditions for each parameter are determined, the robust candidate design is fed into automated script-based protocol to estimate its T_r. The robust design is also exposed to the outer noise trials. This enables the performance to be compared against the main trial performances.

C. Simulation Manager

The script-based *Simulation Manager* block manages the model set-up, updates the design parameters and processes the simulation results as set out by the *Static Step Script*. The function block is detached from the *Taguchi Analysis Tool* to allow the use of different FEA packages. The required data between the two function blocks are shared using data files such as *.txt* or *.csv* files. This further contributes to the parallel machine trial processing capabilities of the framework. The main functionality of the block is driven by the *Static Step Script* which was compiled using [14]. The *Simulation*

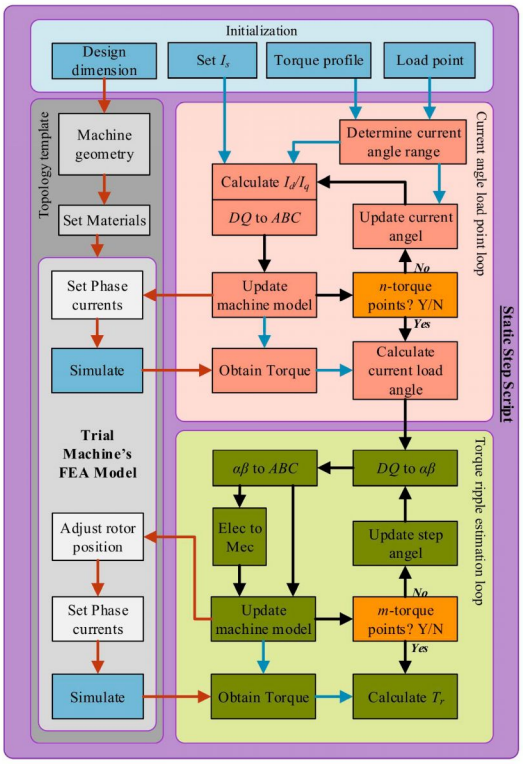

Fig. 3. Functional breakdown of torque ripple estimation framework.

Manager initiates the *Static Step Script*, calculates the T_r and flags the *Taguchi Analysis Tool* to read the calculated value from the required files.

D. Static Step Script

To calculate the T_r of a machine using FEA, a series of specific static steps are required for the relative torque-current angle. The steps represent mechanical rotation over a set angle, usually one stator slot, with the stator excitation electrically adjusted to ensure the required torque angle. To calculate the T_r the static step script uses four function blocks as in Fig. 3, where the black arrows represent direct actions, the blue arrows indicate an informational exchange and red arrows form part of the Topology template script execution of the FEA model.

- ***Initialization:*** The torque profile of the initial design is determined using a *DQ*-current sweep of I_s as done in [14]. The machine's dimensions are obtained from the *Taguchi Analysis Tool* and *Designer Interaction* function blocks which is used to set-up and simulate each candidate machine.
- ***Topology template:*** To enable fast set-up of FEA model for each trial machine, a script-based parametrized model is used. When required, changes are made to the machine geometry and material properties as defined by the *Taguchi Analysis Tool* and then used for the specific design trials. The *Current angle load point* and *Torque ripple estimation* loops interact with FEA model as indicated to obtain the required information.

TABLE I
KEY LS-PMSM DESIGN SPECIFICATIONS

Description	Stator	Rotor
Outer diameter (mm)	160	99.225
Inner diameter (mm)	99.775	26
Stack length (mm)	120	120
Winding type	Lap	Cage
Number of slots	36	28
Turns per slot	41	1
Core material	M400-50A	M400-50A
Magnet type	-	N48H
Rotor bars	-	1050 alloy
Moment of inertia (kg.m^2)	-	0.009

- ***Current angle load point loop:*** Using the original torque profile in conjunction with the selected load point a *DQ*-current angle range is identified.
- ***Torque ripple estimation loop:*** Calculating T_r of a trial machine requires a number of torque values over a torque ripple period. Using a static simulation step approach, the mechanical angle of the rotor is adjusted a number of angle points over the period. The torque value of each position is computed by using Maxwell stress tensor along the air-gap contour. Once all torque points have been obtained the T_r is calculation as:

$$T_r = \frac{T_{max} - T_{min}}{T_{ave}} \times 100\% \quad (1)$$

with T_{max} and T_{min} the maximum and minimum torque values of these points, respectively, and T_{ave} the average torque of all the points. Once the T_r is calculated it is sent to the *Taguchi Analysis Tool*.

III. IMPLEMENTATION OF PROPOSED FRAMEWORK

This section presents the implementation of the proposed framework as described in Section II on the selected base machine. To initialize the framework only the *Design interaction* and *Simulation manager* function blocks have to be set-up. The *Taguchi analysis tool* is dependent on the design array configuration.

A. Machine topology and specification

For the design study a 4-pole, 525 V, 2.2 kW, prototype LS-PMSM is used as the base machine. The machine was initially designed to consider both transient and steady-state performance objectives [1]. The multi-objective design optimization did not include the minimization of T_r which makes the candidate machine ideal for the implementation of the proposed framework. The basic specifications of LS-PMSM are summarized in Table I. The layout of the machine is shown in Fig. 1. The study aims to minimize the torque tipple while keeping the influence to its original performance objective to a minimum.

B. Designer interaction

To ensure minimal impact on the original performance objectives as in [1], dimensional changes are limited only to

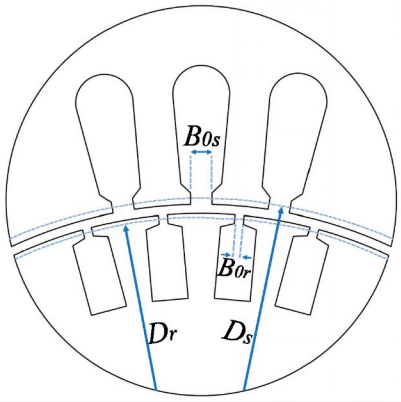

Fig. 4. Selected design parameters for main array.

TABLE II
DESIGN AND NOISE PARAMETER INFORMATION

Design	B_{0r}	B_{0s}	D_s	D_r
Minimum (mm)	0	2	99.725	99.175
Maximum (mm)	2	2.4	99.825	99.275

Noise	Rotor stacking	PM	Load point
State 1	0.93	Minimum	Rated
State 2	0.98	Typical	Peak

the rotor and stator slot openings (B_{0r}, B_{0s}) and air-gap (D_r, D_s) as shown in Fig. 4.

To induce performance variance, noise factors known to influence T_r (or the selected objective) must be used. For the study, the selected noise factors are the PM material variance which influences rotor flux, the lamination stacking factor of the rotor which influences the air-gap surface area and alignment, and lastly the load point as this influences the torque angle. For the PM material variance, the typical and minimum magnetic performance properties are selected which influences the energy product of the magnetic volume (BH_{max}). For the load point noise factor, the peak torque of the motor at rated current will be used. The stator lamination stacking factor is selected as 0.95. Table II contains the information of the selected parameters.

For the main OA an *L9* array can be used. The array uses four 3-level parameters resulting in nine main trials. Table III presents the *L9* main OA with parameters levels, the air-gap length is included for information purposes only. For the noise factors an *L4* OA is used. The array uses three 2-level parameters resulting in four noise trials per main trial. Thus, the total number of trial machines are 36 in addition to four robust machine trial.

C. Simulation Manager

As part of the Simulation manager block initialization, an FEA tool is required. For the implementation, the open source package FEMM [15] is used, which incorporates a band solver to handle the motion in the analysis [16]. By taking advantage of magnetic symmetry, it is only necessary to model one-pole of the machine with negative periodic boundary conditions as in Fig. 1. For the torque ripple calculation per trial design, it requires four torque points to determine the torque-current-angle and 15 steps to calculate the torque ripple. The total time required to execute all 40 machine models (760 simulations) was approximately 7 hours without the use of parallel model computing using an Intel core i7 3.5 GHz processor.

TABLE III
L9 MAIN DESIGN ARRAY

L9	B_{0s}	B_{0r}	D_s	D_r	Air-gap = $D_s - D_r$
T1	2.4	2	99.825	99.275	0.55
T2	2.4	1	99.775	99.225	0.55
T3	2.4	0	99.725	99.175	0.55
T4	2.2	2	99.775	99.175	0.60
T5	2.2	1	99.725	99.275	0.45
T6	2.2	0	99.825	99.225	0.60
T7	2	2	99.725	99.225	0.50
T8	2	1	99.825	99.175	0.65
T9	2	0	99.775	99.275	0.50

IV. RESULTS

Table IV summarizes the original and final design parameters together with their respective performances. The power factor, efficiency and line current were calculated as in [1] and the normalized critical inertia (x_{cr}) estimated as in [17]. The final design has a reduced stator slot opening, a closed rotor slot and an increased air-gap, which are in-line with the published results in [2]–[4], [6]. When comparing the steady-state performance between the two designs, a slight decrease in power factor and efficiency is noted, resulting in an increase in the line current as shown. The decrease in power factor is attributed to the increase in rotor leakage flux caused by the closed rotor slots. This, however, reduces the braking torque leading to an increased x_{cr}. Fig. 5 compares the x_{cr} as a function of the percentage rated load as commonly found in literature. The increase in x_{cr} is evident over the larger load percentage range. With regards to T_r near rated load, a reduction of 61.04% was achieved whereas at peak load a reduction of 18.72% with only a 2 N.m decrease in peak torque. Using the information obtained, the T_r graph over one stator slot torque period can be compiled. Fig. 6 and Fig. 7 present the two operating points (rated and peak load respectively) for observation as part of the robust optimization. The figures include the original machines T_r (T_rOri), the robust machine (T_rOpt) and their respective averages (T_{ave}Ori, T_{ave}Opt). Noted in both figures are significant decreases in T_r for both rated and peak loads.

A. Taguchi Optimization

The robust optimum parameters in Table IV were identified using the ANOM analysis. Although it is done mathematically, the information can be visually represented as in Fig. 8 with the robust parameter levels as indicated by the enlarged dots. The lines between the levels represent the effect on the objective as the parameter is increased or decreased. The gradient of the line between two points indicates the effective degree of performance change due to the parameter change.

TABLE IV
COMPARISON OF DIMENSIONS AND PERFORMANCE BETWEEN THE ORIGINAL AND ROBUST DESIGNS

Description	Original	Robust
B_{0s} (mm)	2.4	2
B_{0r} (mm)	1	0
D_s (mm)	99.775	99.825
D_r (mm)	99.225	99.225
Air-gap (mm)	0.55	0.60

Calculated Performance	Original	Robust
Power factor	0.81	0.78
Efficiency (%)	89.21	88.79
Line current (A)	3.20	3.34
T_r at rated torque (%)	83.26	22.22
T_r at peak torque (%)	31.47	12.75
Rated x_{cr}	12.34	13.21

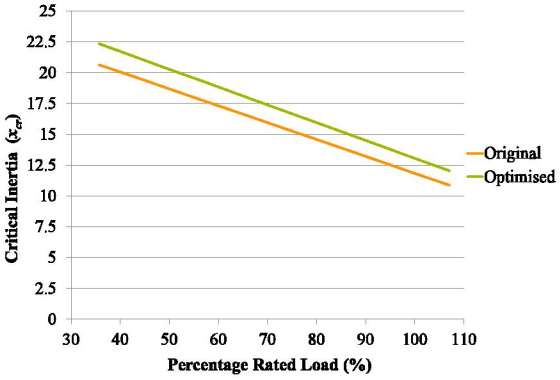

Fig. 5. Critical inertia comparison as a function of rated load.

This in conjunction with the ANOVA gives useful information on the influence and susceptibility of a parameter to external noise factors. Considering this, the most significant reduction in T_r was archived by changing B_{0r} from level 2 to level 3 and is confirmed by the ANOVA as shown in Fig. 9.

Although the ANOM gives indication on the degree of change, the ANOVA can provide the magnitude. This is done by calculating the percentage contribution of a specific

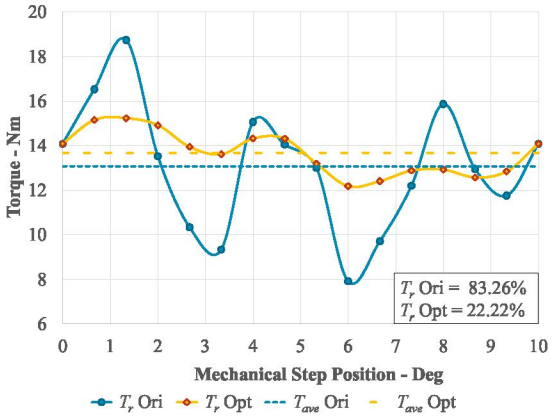

Fig. 6. Torque ripple comparison at rated performance over one stator slot.

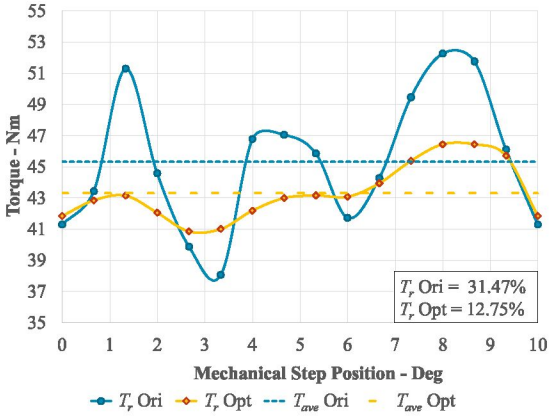

Fig. 7. Torque ripple comparison at peak performance over one stator slot

parameter toward performance variance on the main trials as a function of the selected noise parameters. This information can be used to identify the most influential parameter and reduce the number of parameters by discarding the least influential ones. Fig. 9 confirms that B_{0r} is the most significant contributor to performance variance with D_s also having a notable influence. The information obtained from the ANOVA can also be used to set stricter manufacturing specifications to parameters or areas that have a more significant influence on performance variance.

The main trial results are presented in Fig. 10 and Fig. 11. The values expressed in the bar-graph is in terms of the calculated S/N ratio due to the use of the outer noise. Thus, the T_r values presented in Fig. 11 is the S/N ratio value converted back and represents the logarithmic combined values of the noise trials and should not be seen as the average [10]. This value provides a better performance expectation. Indicated on the graph is the original and optimum trial values which indicate the reduction in T_r. The graphs also make it easy to visually inspect if the robust optimum machine is truly better as the Taguchi method is susceptible to inter-dependent parameter influence. If interdependency is present, the ANOVA's calculation error will confirm this. When using the proposed method for a sensitivity analysis, a low trial variance indicates the optimum design is located in a stable region. The high variance in Fig. 10 and Fig. 11 indicates that a second round optimization is required. For this, the parameter ranges should be reduced by considering the information in Fig. 8.

V. CONCLUSION

In this paper a robust mitigation framework has been proposed that can effectively reduce the ripple torque of an LS-PMSM. The proposed framework was successfully implemented on a previously designed LS-PMSM. The robust design was realized with only considering nine main machine candidates to reduce the torque ripple by 61.04% and 18.72% at the selected operating points, respectively. Considering the notable decrease in torque ripple at both load points without significant reduction in both steady-state and transient load

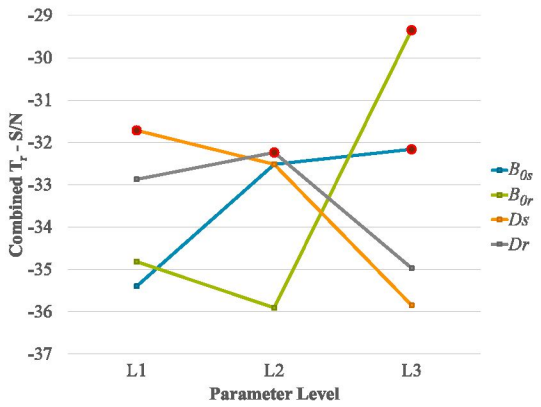

Fig. 8. ANOM parameter level effect plots on torque ripple.

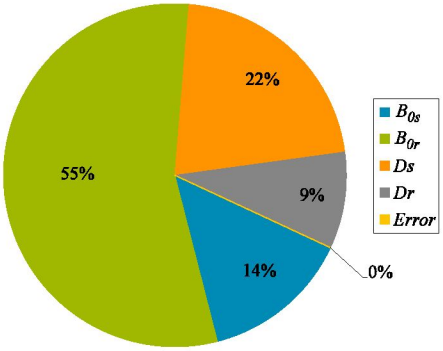

Fig. 9. ANOVA parameter percentage contribution to torque ripple variance.

synchronization capabilities, the proposed robust mitigation framework can be deemed as a viable method. A key advantages of the Taguchi method based robust design framework is the ability to identify and quantify the performance variance whiles realizing the best suited design. When compared to traditional optimization techniques, the proposed robust design framework is independent from the designers' input in realizing the robust design whereas traditional approaches relies on the designers interpretation of the results.

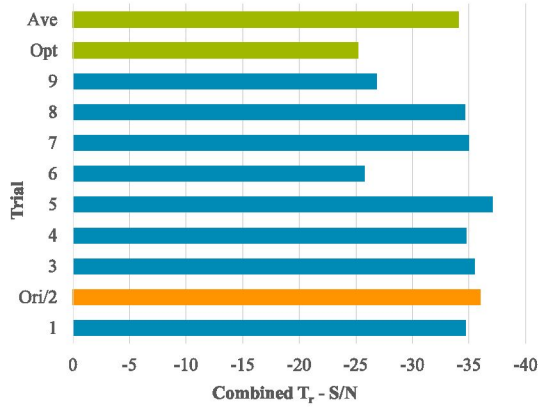

Fig. 10. Torque ripple trial variance plot - S/N ratio due to outer noise trials.

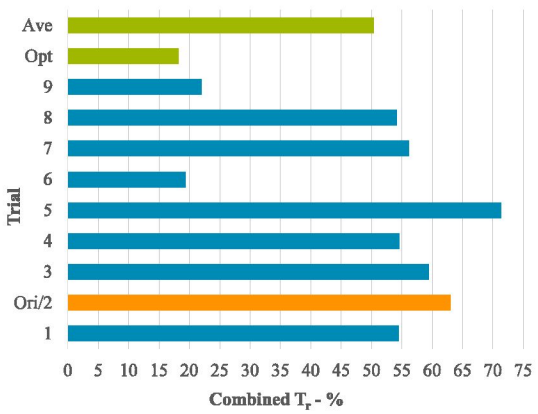

Fig. 11. Torque ripple trial variance plot - Converted S/N rations of Fig. 10.

REFERENCES

[1] A. J. Sorgdrager, R-J. Wang and A. J. Grobler, "Multiobjective design of a line-start PM motor using the Taguchi method," *IEEE Transactions on Industry Applications*, 54(5): 4167-4176, Sept.-Oct. 2018.

[2] B. Gaussens, J. Boisson, A. Abdelli, L. Favre and D. Bettoni, "Torque ripple mitigation of PM-assisted synchronous reluctance machine : Design and optimization," 20th International Conference on Electrical Machines and Systems (ICEMS), Sydney, NSW, 2017, pp. 1-6.

[3] N. Bianchi, M. Degano and E. Fornasiero, "Sensitivity analysis of torque ripple reduction of synchronous reluctance and interior PM motors," *IEEE Transactions on Industry Applications*, 51(1): 187-195, Jan.-Feb. 2015.

[4] T. M. Jahns and W. L. Soong, "Pulsating torque minimization techniques for permanent magnet AC motor drives-a review," *IEEE Transactions on Industrial Electronics*, 43(2): 321-330, April 1996.

[5] E. Howard, M. J. Kamper and S. Gerber, "Asymmetric flux barrier and skew design optimization of reluctance synchronous machines," *IEEE Transactions on Industry Applications*, 51(5): 3751-3760, Sept.-Oct. 2015.

[6] S. Monjezi, A. Kiyoumarsi, B. M. Dehkordi, M-F. Sabahi, M-H. Vafaie, "Shape design optimization of interior permanent-magnet synchronous motor with Machaon flux barriers for reduction of torque pulsation", *Electric Power Components and Systems*, 44(19): 2212-2223, 2016.

[7] M. Si, X. Y. Yang, S. W. Zhao, S. Gong, "Design and analysis of a novel spoke-type permanent magnet synchronous motor". *IET Electric Power Applications*, 10(6): 571-580, 2016.

[8] W. Ren, Q. Xu and Q. Li, "Asymmetrical V-shape rotor configuration of an interior permanent magnet machine for improving torque characteristics,"*IEEE Transactions on Magnetics*, 51(11): 8113704, Nov. 2015.

[9] A. J. Sorgdrager, R-J. Wang, and A. J. Grobler, "Taguchi method in electrical machine design," *SAIEE African Research Journal*, 108(4): 150-164, Dec. 2017.

[10] R. Roy, *Design of experiment using the Taguchi approach*, Wiley, New York, 2001.

[11] K. Kim, "A novel method for minimization of cogging torque and torque ripple for interior permanent magnet synchronous motor," *IEEE Transactions on Magnetics*, 50(2): 793-796, Feb. 2014.

[12] W. Ren, Q. Xu, Q. Li and L. Zhou, "Reduction of cogging torque and torque ripple in interior PM machines with asymmetrical V-type rotor design," *IEEE Transactions on Magnetics*, 52(7): 8104105, July 2016.

[13] K. S. Kim, K. T. Jung, J. M. Kim, J. P. Hong, S. I. Kim, "Taguchi robust optimum design for reducing the cogging torque of EPS motors considering magnetic unbalance caused by manufacturing tolerances of PM." *IET Electric Power Applications*, 10(9): 909-915, 2016.

[14] N. Bianchi, *Electrical machine analysis using finite elements*, CRC press, 2005.

[15] D. Meeker, "FEMM 4.2." http://www.femm.info/wiki/HomePage

[16] D. Meeker, "Sliding band motion model for electric machines", http://www.femm.info/wiki/SlidingBand, March 2018

[17] A. Chama, A. J. Sorgdrager and R-J. Wang, "Analytical synchronization analysis of line-start permanent magnet synchronous motors." *Progress In Electromagnetics Research M, (PIER M)*, 48: 183-193, 2016.